NJC

Accepted Manuscript

This is an *Accepted Manuscript*, which has been through the Royal Society of Chemistry peer review process and has been accepted for publication.

Accepted Manuscripts are published online shortly after acceptance, before technical editing, formatting and proof reading. Using this free service, authors can make their results available to the community, in citable form, before we publish the edited article. We will replace this *Accepted Manuscript* with the edited and formatted *Advance Article* as soon as it is available.

You can find more information about *Accepted Manuscripts* in the Information for Authors.

Please note that technical editing may introduce minor changes to the text and/or graphics, which may alter content. The journal's standard Terms & Conditions and the Ethical guidelines still apply. In no event shall the Royal Society of Chemistry be held responsible for any errors or omissions in this *Accepted Manuscript* or any consequences arising from the use of any information it contains.

ROYAL SOCIETY OF CHEMISTRY

www.rsc.org/njc

New Journal of Chemistry

RSCPublishing

ARTICLE

Scratch resistant sol-gel coatings on pristine polycarbonate

Cite this: DOI: 10.1039/x0xx00000x

Nicolas Le Bail,[a,b] Krystelle Lionti,[c]* Stéphane Benayoun,[a] Sophie Pavan,[a] Leslie Thompson,[c] Christel Gervais,[d] Géraud Dubois,[c] Bérangère Toury[b]*

Received 00th January 2012,
Accepted 00th January 2012

DOI: 10.1039/x0xx00000x

www.rsc.org/

The deposition of protective transparent coatings on polycarbonate (PC) with higherscratch resistance than the polymeric substrate is performed using an original sol-gel system. Our strategy relies on the preparation of hybrid organic-inorganic (HOI) films by sol-gel, based on 3-glycidoxypropyltrimethoxysilane (GPTMS), tetraethoxysilane (TEOS) and zirconium (IV) propoxide (ZTP). We show that, despite a low coating to PC adhesion (<2J/m^2), it is possible to maintain the coating integrity under high applied scratch forces when the organic domains of the film are highly connected. In this case, the increase in organic network connectivity was achieved through the reaction of epoxide rings in presence of ZTP, as evidenced by FTIR. The subsequent additional plasticity of the coating led to an increase in scratch-test delamination force by more than twofold: from 1.7 N for the hybrid film without ZTP to 3.8 N with the highest ZTP content. Regarding the inorganic network, an increasing number of Si-O-Zr and Zr-O-Zr bonds with increasing ZTP content was evidenced by FTIR and ^{17}O MAS NMR, allowing improved hydrolysis resistance and therefore more durable coatings. Altogether, these results demonstrate the key role played by ZTP in tuning the HOI coating's mechanical properties and durability without requiring adhesion promoting treatments.

Introduction

Transparent polymers, such as PC, are used commercially in a broad range of applications, from automotive windows to optical lenses. Nevertheless, it was early on recognized that PC suffers from chemical and mechanical weaknesses that can significantly reduce its transparency and performance. In the first case, its permeability to O_2 and H_2O combined with UV-irradiation or humid environment[1–4] lead to the release of bisphenol A (BPA), a molecule of concern for human health. From a mechanical point of view, PC presents a high resistance to impact and fracture but due to its very low surface hardness can be easily scratched (first scratch appears at 0.2 N using a 200µm tip radius).[5] Among the different strategies envisioned to mitigate these issues, silicon oxide-based hard coatings have also been deposited onto PC by physical vapor deposition (PVD),[6,7] plasma-enhanced chemical vapor deposition (PECVD)[8–10] and atmospheric plasma.[11,12] Using these deposition methods, a compromise between the coating bulk and interfacial properties is usually achieved.[12] Conversely, pre-treating polymers with a plasma source to activate the substrate[11] or to deposit an intermediate adhesive layer[13] enables an independent control of these mechanical properties. Interestingly, the former approach is not specific to gas phase deposition techniques but was also successfully implemented with sol-gel coatings. For example, the adhesion to PC of sol-gel coatings based on GPTMS, TEOS and silica nanoparticles increased by a factor of 10 after a N_2/H_2 plasma treatment while the Young's modulus remained above 8 GPa. However, the coating brittleness was found to be the limiting factor to resist to scratch loads higher than 1.8 N.[5] It is worth noting that this observation appears to hold true for most scratch resistant sol-gel systems reported in the literature. For example, coatings based on TEOS and diethylenetriamine (DETA), or SiO_2/TiO_2 mixed oxides cured by thermal means or using microwaves[14], tend to easily crack[15] and even delaminate if the film adhesion is low. To avoid film cracking, resins such as epoxy[16], acrylate oligomer[17,18] or polyethylene oxide[19] are often incorporated in the sol-gel network to increase the overall coating plasticity. Unfortunately, the increase in organic content leads to lower hardness and scratch resistance.

We believe that a coating displaying higher plastic properties should not necessarily require high adhesion to PC as well as high hardness to provide good mechanical protection. In this paper, transparent and homogeneous hybrid coatings atop PC were prepared by dip-coating from sols containing GPTMS, TEOS, silica nanoparticles and varying amount of ZTP (Zr/Si ratio ranging from 0 to 0.33). The zirconium alkoxide acts as an efficient catalyst for epoxide ring opening[20–22] leading to the formation of longer carbon chains in the network, imparting additional plastic properties to the film. As expected, Double Cantilever Beam (DCB) measurements confirmed that the adhesive energy is independent from the sol composition and is well below values reported for similar Zr-free sol-gel coatings

on treated PC.[23] Contrastingly, delamination force values measured during scratch test were significantly superior for the Zr-based coatings and increased as the function of the Zr/Si content to reach 3.8 N for the highest Zr/Si ratio. Changes in the chemical network were studied using IR spectroscopy indicating that the epoxide groups from GPTMS are efficiently opened even at low Zr/Si ratio. Interestingly, with an increasing Zr content, more Si-O-Zr and Zr-O-Zr bonds are introduced in the film. Their beneficial impact to the coating mechanical properties was further evaluated by nanoindentation measurements, showing an excellent agreement with the scratch tests. In essence, we show that despite low adhesion and surface hardness, good scratch resistance can still be achieved by tuning both the organic and inorganic networks through the chemical composition (ie Zr/Si ratio).

Experimental section

Materials

3-glycidoxypropyltrimethoxysilane (GPTMS), tetraethoxysilane (TEOS), zirconium (IV) propoxide solution at 70wt% in *n*-propanol (ZTP), hydrochloric acid (HCl), isopropanol (IPA) and methacrylic acid (MAA) were purchased from Sigma-Aldrich. Colloidal silica (Levasil 200E with particle sizes of 10-80 nm, 20 wt% solid content, suspension in water) was generously given by Akzo Nobel. All the chemicals were used as received, without any further purification. 2mm-thick bisphenol A-polycarbonate sheets (Lupilon S3000 UR) were provided by Mitsubishi Corp.

Hybrid sol-gel coating preparation

Solution A was prepared by mixing and stirring GPTMS:TEOS:HCl:IPA in the following molar ratios: 5:1:0.2:3.3. When solution A became transparent, Levasil 200E was added under stirring (in an amount such that the colloidal silica dry extract in the coating after curing is 20 wt%). This system with no ZTP is referred to as Z0. Then, solution B was prepared by mixing ZTP:MAA in the molar ratio 1.5:1, and stirred for 20min at RT. MAA was used to react with ZTP and form a complex.[24] Solutions B was consecutively added to solution A very slowly, in four different Zr/Si molar ratios: 0.12, 0.23, 0.35 and 0.48. These systems are respectively referred to as Z1 (low Zr content), Z2, Z3 and Z4 (high Zr content). The five systems were then kept under vigorous stirring.

Coating method and curing

PC slabs (50 mm x 25 mm) were cleaned with distilled water and degreased with ethanol prior to film deposition. They were subsequently coated using the dip-coating method (adjusting the withdrawal speed to obtain the desired thickness) and referred to as PC-Zx with x=0,1,2,3 or 4, depending on the solution used. After coating deposition, the samples were cured in a ventilated oven at 135°C for 1 h. It is worth mentioning that this temperature is below the PC glass transition temperature, to preserve PC mechanical cohesion.

Characterization

Film thickness was measured by profilometry (Dektak, Veeco) at the raw/coated PC interface. The coatings scratch resistance and adherence were evaluated by scratch-test (Micro Scratch Tester, CSM) using a Rockwell indenter (tip radius = 200 µm) moving along the surface at a rate of 5mm/min, applying a force increasing by increments of 0.2 N, from 0 to 5 N. All the samples were tested five times and the experimental error is always less than 0.15 N.

The coatings density was measured by X-ray reflectivity (XRR) using an X'Pert ProMRD diffractometer (Panalytical, Westborough, MA) with a ceramic X-ray tube (λ = 0.154 nm) and a high resolution horizontal goniometer (reproducibility = ± 0.0001°).

Infrared spectra were recorded with an FTIR 300E spectrometer (Jasco, France) in attenuated total reflectance (ATR) mode, in the range [500 - 4000] cm^{-1}.

The coatings adhesion energy on PC was quantified using the symmetric Double Cantilever Beam (DCB) test. The specimens were prepared by bonding a blank (uncoated) substrate of 2 mm- thickness (surface 1) onto a coated substrate of the same thickness (surface 2). The fracture tests were conducted on a micromechanical adhesion test system (DTS Delaminator Test System, DTS Company, Menlo Park, CA) in displacement control mode. More information about this technique can be found elsewhere.[23]

Nanoindentation measurements were carried out on a Nanoindenter XP from MTS Corporation that has been described elsewhere.[25] A Berkovich indenter with a face angle of 115.12° was employed. In addition to the static depth sensing procedure, a dynamic harmonic load oscillation of small amplitude (1.5 nm) at a frequency of 32 Hz was used. The load on the sample was recorded as a function of the indenter displacement into the sample's surface. Hardness and Young's modulus could thereafter be determined as a function of the penetration depth.

Changes in the coatings inorganic network were monitored using ^{17}O solid-state NMR. Bulk samples Z1-^{17}O, Z2-^{17}O, Z3-^{17}O and Z4-^{17}O were prepared in the same experimental conditions with enriched a 10% enrichment ^{17}O water (Sigma-Aldrich). The resulting sols are then cured at 135°C to finally be transformed in powder. Experiments were performed at high magnetic field on a 700 MHz AVANCE III Bruker spectrometer operating at 94.89, using a 4 mm low gamma Bruker probe spinning at 10 or 14 kHz (both spinning speeds were used for each samples to determine precisely the position and intensity of the spinning sidebands). A spin-echo θ-τ-2θ pulse sequence with θ = 90° was chosen to overcome probe ringing issues and baseline distortions. The τ delay was synchronized with the spinning frequency.

XPS analysis was done on a Physical Electronics Quantum 2000 ESCA Microprobe, using a monochromated AlK_a X-ray source (1486 eV), 200 µm spot size throughout and charge neutralization. 0-1000 eV range survey spectra (187 eV pass energy, 1.6 eV/step) and high resolution spectra (47 eV pass energy, 0.4 eV/step) were taken. High resolution spectra were referenced to $C(1s)_{max}$ = 284.8 eV. The angle between the detector and sample surface was 45 degrees. Depth profiles were obtained using an Ar sputter gun at 3kV for 2 minutes per cycle with a 3x3mm spot size, for a total of 550 cycles.

SEM images were obtained using a Scanning Electron Microscope operating at 10 and 15 kV (FEI QUANTA 250 FEG, SDD Bruker detector).

The water vapor resistance of the coatings was assessed by placing 1 cm^2 of coated PC in a water vapor environment (100% humidity) and evaluating the minimum time leading to film decohesion. Wettability was estimated by water contact angle (DSA30, Krüss).

Results and Discussion

Processing conditions

The sol gel process under acidic conditions was used to prepare a series of transparent ZrO_2/SiO_2 based coatings on PC with different Zr/Si ratio ranging from 0 to 0.48. It is worth pointing out that Levasil 200E (colloidal silica) was used as a filler, to reinforce the sol-gel coatings cured at a relatively low temperature (135°C).[5,26] Since the coatings mechanical and/or adhesion properties can be impacted by the film thickness,[27] the latter was fixed to 4 µm for all films by adjusting the withdrawing dip-coating speed, allowing for a direct comparison of the coatings properties. All coatings were deposited after 24 h of sol aging to ensure complete hydrolysis of the precursors while condensation is only initiated, as evidenced by Nuclear Magnetic Resonance (NMR) analysis.[28] In that case, condensation mainly takes place during and after coating deposition, directly on the PC substrate. As a first step, the coatings composition and homogeneity were assessed by XPS. The impact of the increasing ZTP content on the coating scratch-resistance properties was then evaluated by scratch-test. Complementary characterizations by DCB, FTIR, nanoindentation and XRR were also performed to understand the role of ZTP in the coatings chemical and structural modification.

Coating composition and homogeneity

First, surface elemental composition of PC-Z1, PC-Z2, PC-Z3 and PC-Z4 were determined by XPS to evaluate the coatings homogeneity. Figure 1 shows the profile of PC-Z3. The contribution of each of the four elements detected (C1s, O1s, Si2p and Zr3d) is constant throughout the whole film thickness, indicating very high bulk homogeneity.

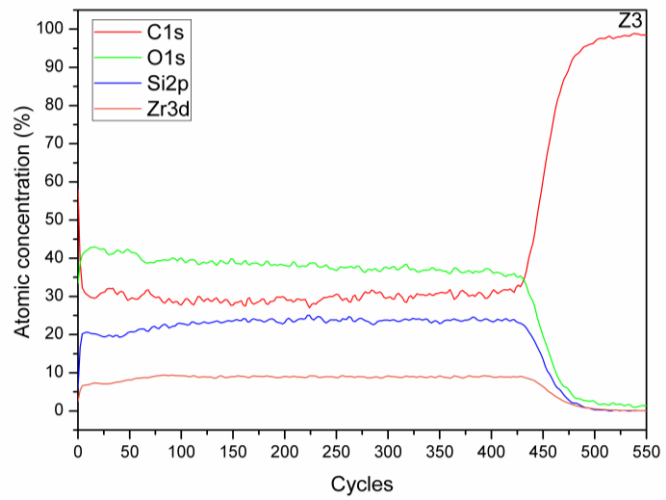

Fig 1 XPS profile obtained on PC-Z3

Similar profiles were obtained on PC-Z1, PC-Z2 and PC-Z4 and can be found in supporting information (figure SI1). Based on these profiles, the experimental Zr/Si atomic ratios were calculated and reported in Table 1, along with the theoretical ratios. Second, SEM images recorded on all samples confirmed the homogeneity in both film surface and cross-section (figure SI2). Additionally, an excellent match in film thickness was obtained between values from profilometry and those measured on the SEM cross-section images.

Table 1 Experimental and theoretical Zr/Si atomic concentration ratios of the coatings as measured by XPS

	XPS values	Theoretical values
PC-Z1	0.13 ± 0.01	0.12
PC-Z2	0.18 ± 0.01	0.23
PC-Z3	0.38 ± 0.02	0.35
PC-Z4	0.50 ± 0.03	0.48

As expected, the Zr/Si ratio increases when the ZTP quantity is increased. Moreover, the experimental and theoretical values are in excellent agreement, indicating that no phase separation occurred during coating preparation, as observed in some cases as a function of dip-coating conditions.[28] Altogether, these preliminary results demonstrate the successful incorporation of ZTP within the bulk and a good chemical homogeneity of the films.

Film/PC interfacial adhesion

Adhesive fracture energy measurements were then conducted on PC-Z1, PC-Z2, PC-Z3 and PC-Z4 by DCB. This technique was recently tested on silica based coatings on PC and allows for interfacial adhesion measurements independently of any other mechanical characteristic.[23,29] It permits to measure the adhesion in $J.m^{-2}$ (Gc) by applying loads/unloads at a controlled displacement rate to produce coating cracks growth. It is worth mentioning that the fracture path was examined for all four samples using x-ray photoelectron spectroscopy (XPS). For clarity purposes, only XPS data of PC-Z4 are reported (Table 2) as these of PC-Z1 to PC-Z3 are similar and lead to the same conclusion.

Table 2 Composition of surface 1 and surface 2 of PC-Z4 after DCB test, as measured by XPS

Sample / atomic pourcentage (%)	C(1s)	O(1s)	Si(2p)	Zr(3d)
Surface 1 (initially PC blank)	56.2	32.5	9.5	1.8
Surface 2 (initially displaying coating)	77.0	19.0	4.0	0.0

The composition of surface 1 after DCB test displays a high Si atomic percentage along with a low percentage of Zr. Thus, it corresponds to that of the coating. With regards to surface 2, initially being the coating (on top of PC), the absence of Zr combined with the calculated C/O ratio (4.1) being quite close to the theoretical ratio for PC (5.2) show that surface 2 becomes PC after DCB test. Altogether, these results indicate that the fracture occurred at the film to PC interface, evidencing the adhesive nature of the fracture.
The adhesive fracture energy G_c measure on each sample is reported in Table 3.

Table 3 Coatings adhesive fracture energy as measured by DCB

Sample	PC-Z1	PC-Z2	PC-Z3	PC-Z4
G_c (J/m^2)	1.5 ± 0.4	2.2 ± 0.6	2.5 ± 0.3	1.7 ± 0.5

The G_c values measured were all in the range 1.5-2.5 J/m^2, irrespective of the ZTP content. It is worth noting that, in light of their standard deviation, these four G_c values are considered as similar. Moreover, these low values below 3 J/m^2 are indicative of few or no covalent bonds at the interface between

the coating and the PC. Indeed, when covalent bonds are present between a similar Zr-free coating and PC, it was shown that G_c can be as high as 22 J/m^2, as plasticity from both PC and coatings are getting activated. In the present case, the crack propagated at low applied stress and consequently little energy was dissipated, leading to low G_c values. These results were expected as no PC surface activation was done prior to coating deposition, and they are in excellent agreement with previous G_c values measured on silica-based sol-gel coatings on untreated PC.[23]

Scratch resistance

Scratch-tests were performed on PC-Z0, PC-Z1, PC-Z2, PC-Z3 and PC-Z4 to assess the effect of ZTP on the coatings scratch-resistance: optical microscopy images of the five samples, at different loads, are presented in Figure 2. Each sample was tested five times: the results were extremely reproducible as the experimental error on the critical loads was always less than 0.15 N. It is worth pointing out that scratch-test results are a function of both bulk mechanical properties and interfacial adhesion, as the indenter stresses the coatings normally and tangentially at the same time. However in this case, all samples display similar low adhesion energies as demonstrated by DCB; therefore, any differences observed in scratch resistance can be directly ascribed to differences in bulk structure and/or composition. It should also be noted that the low coating to PC adhesion measured by DCB is also visible on the scratch images from the crack occurring beyond the contact surface (i.e outside of the groove dug by the indenter) that propagates at the interface.

The coatings behavior under scratch stress varies upon the ZTP content. Regarding the Zr-free coating (PC-Z0), cracks formed first (F=1.1 N) and delamination took place at a higher force (1.7 N). In the case of zirconia containing samples, no damage (cracks or scales) occurred until film delamination was reached. Moreover, at the critical force, the groove width of PC-Z0 is thinner than that of PC-Z1, PC-Z2, PC-Z3 and PC-Z4 which all display a similar groove width. The latter observation could indicate that the incorporation of zirconia leads to more ductile coatings, and this hypothesis will be confirmed further in the paper by the nanoindentation data. Another interesting observation is the gradual increase in critical load (lower force at which film damage occurs) from 1.1N for PC-Z0 to 3.8 N for PC-Z4, indicating that a better scratch resistance is obtained when ZTP is introduced in the coatings, especially with a high ZTP content. It is worth pointing out that the fourfold increase in scratch resistance reaching a delamination value of 3.8 N when ZTP is added to a silica-based sol-gel coating is a very high scratch resistance on untreated PC. These results are direct consequences of the coating chemical modifications imparted by the ZTP, and two simultaneous phenomena can be invoked to explain them: i) an increase in Young's modulus and hardness due to Si-O-Zr and Zr-O-Zr bond formation in the inorganic network ii) more plasticity from the organic domains due to the catalytic effect of ZTP on epoxy ring opening which leads to a more polymerized organic network. In order to better understand the impact of network modification imparted by the ZTP on the films mechanical properties, additional characterizations by nanoindentation and x-ray reflectivity were then carried out on all samples.

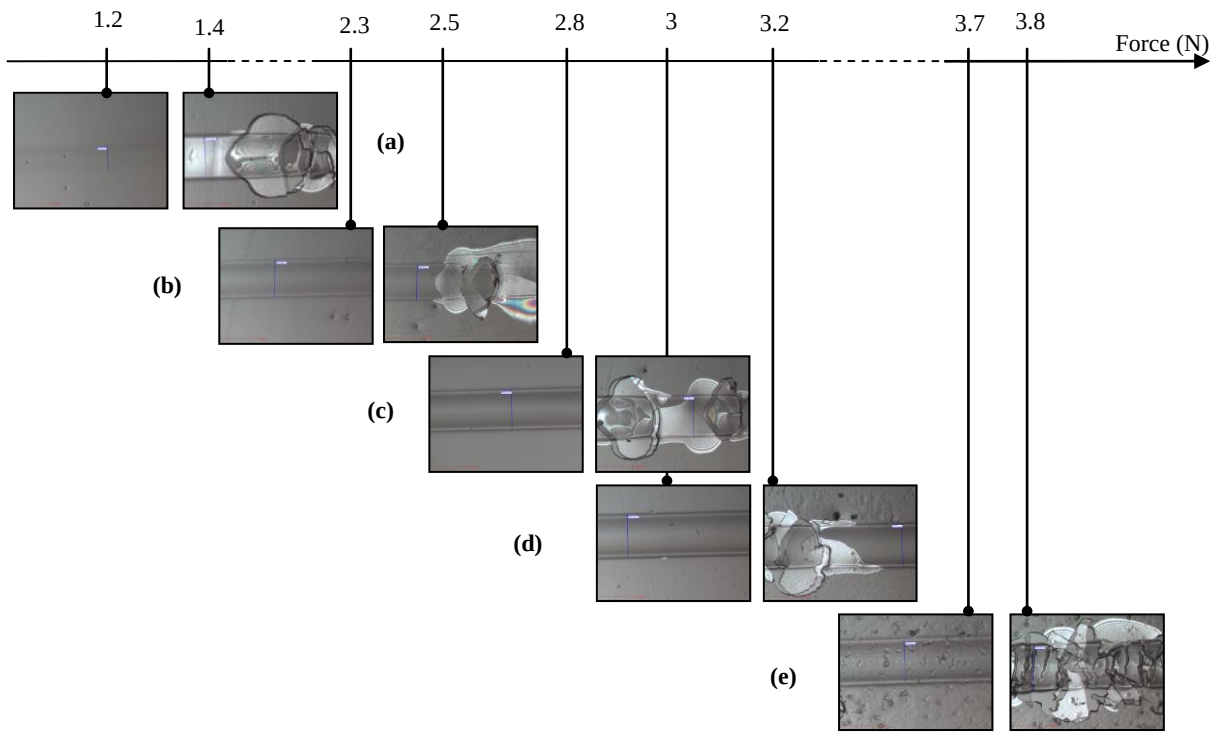

Fig 2 Scratch-test images of coatings with different Zr/Si ratio (a) PC-Z0, (b) PC-Z1, (c) PC-Z2, (d) PC-Z3 and (e) PC-Z4 (Picture size : 450µm x 600µm)

Mechanical properties and density

The coatings Young's modulus (E) and hardness (H) were determined by nanoindentation. Dynamic measurements on the different films were performed: by adjusting the amplitude of the dynamic load oscillation (superimposed to the static load signal), hardness and Young's modulus of both the films (low amplitude, to minimize substrate effect) and the PC substrate

(high amplitude) could be determined. For each sample, 5 spots evenly spaced on the surface were probed by the indenter. Raw data recorded on PC-Z1 are shown in Figure 2. The loop (two cycles of load and unload, Fig 3a) allows to verify the reproducibility of the material behavior (in particular the fact that there is no influence of the roughness) by comparing the similarity of the unload curves. Finally, an indentation with high depth allows to verify the substrate characteristics in the highest depths which confirm the quality of the measurements (fig 3).

For reproducibility purposes, five measurements were conducted on each sample: similar curves were obtained, attesting of excellent sample quality. The contact stiffness as a function of plastic depth (hr') was linear within the first 300 nm, indicating that in that range, the indenter response was primarily due to the coating (no substrate effect) and that the coating is highly homogenous.[30] Young's moduli and hardness determined on the different samples are reported in Table 4.

Table 4 Hardness, Young's modulus and H/E ratio of coated and uncoated PC, as measured by nanoindentation

Surface	H (GPa)	E (GPa)	H/E
PC	0.15	3.0	-
PC-Z0	0.90	5.8	0.155
PC-Z1	0.04	0.8	0.050
PC-Z2	0.06	1.4	0.043
PC-Z3	0.10	2.1	0.048
PC-Z4	0.15	3.0	0.050

Superior E and H were obtained when a hybrid silica film (PC-Z0) was deposited atop PC: the Young's modulus doubled while the hardness increased by a factor of four. These results can of course be attributed to the higher mechanical properties of SiO_2 as compared to those of PC, and are in excellent agreement with the results previously reported by other groups on similar systems.[5,15,19,31,32] Interestingly, when a small amount of ZTP was introduced in the system (PC-Z1), both hardness and Young's modulus values drastically dropped. When the ZTP amount was further increased (PC-Z0 to PC-Z4), both characteristics gradually increased. Nevertheless, the final hardness and Young's modulus of the highest ZTP content sample (PC-Z4) remain lower than these of the Zr-free coating. Altogether, these nanoindentation data give strong evidence of network modifications and demonstrate that the coatings mechanical properties were impacted differently, depending on the ZTP content. When a small amount of ZTP was introduced (PC-Z1), one hypothesis to explain the drop in Young's modulus and hardness measured is that the film displays more plasticity. This could be a result of both the greater organic content as MAA is introduced proportionally to ZTP, and the higher degree of polymerization of the organic network if epoxy ring opening occurs. As the ZTP quantity is further increased (from PC-Z1 to PC-Z4), the increasing E and H are indicative of stiffer coatings, deriving from zirconia-type bonds formation (Zr-O-Zr and Si-O-Zr) as the Young's modulus of zirconia is 3 to 4 times superior to that of silica.[33] These Young's modulus and hardness values are nevertheless quite low for sol-gel coatings, especially compared to those of the Zr-free coating PC-Z0, suggesting that the organic network modification due to the addition of ZTP mitigates the increase in mechanical properties.

Finally, we also assessed the ductile behavior of the Zr-containing coatings using the H/E ratio (calculated from nanoindentation).[34,35] This ratio was found lower for the Zr-containing coatings than for the Zr-free one (table 4). Therefore, the H/E ratio combined with the scratch test results clearly indicate that the incorporation of zirconia leads to more ductile coatings.

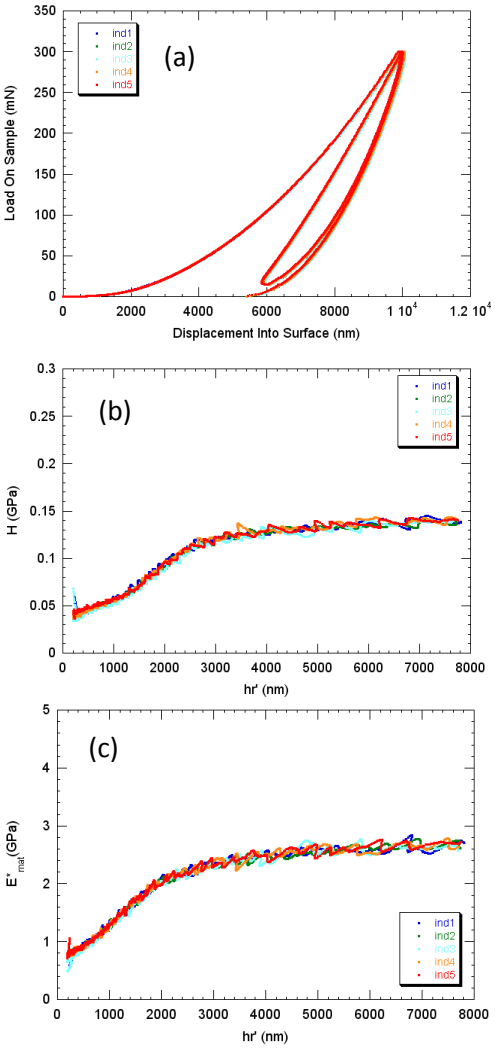

Fig 3 Nanoindentation data as measured on PC-Z1 (a) load –unload curves (b) hardness and (c) Young's modulus as a function hr'(plastic depth)[36,37]

Density measurements by XRR were then carried out on all samples. For each sample, the critical angle and the corresponding density value are reported in Table 5. It is worth mentioning that no Kiessig fringes were observed on the XRR scans due to a high film thickness (4µm).

Table 5 Density as measured by XRR on raw PC, PC-Z0, PC-Z1, PC-Z2, PC-Z3 and PC-Z4

Surface	Critical angle (deg)	Density ($g.cm^{-3}$)
PC	/	1.20
PC-Z0	0.185	1.61
PC-Z1	0.159	1.20
PC-Z2	0.152	1.10
PC-Z3	0.152	1.10
PC-Z4	0.142	0.96

It was anticipated that the evolution of the coatings density would follow the same trend as that of the Young's modulus and hardness, as it is traditionally observed for sol-gel coatings. An increase in density from 1.20 g/cm^3 to 1.61 g/cm^3 was

effectively observed when the PC substrate was coated with a silica based coating, which is in excellent agreement with the literature.[38,39] Although 1.61 g/cm^3 can seem relatively low for a silica based coating, it is in fact a fairly high density value for a HOI silica film annealed at low temperature (135˚C, to remain below the PC's T_g). Following ZTP addition, an important drop in density was observed, supporting the enhancement in organic network imparted by the ZTP, already observed by nanoindentation. However, with higher ZTP content, the density does not follow the same trend as E and H as it continues to decrease and reaches a value about 40% lower than that of the Zr-free film (1.61 g/cm^3 for PC-Z0 vs 0.96 g/cm^3 for PC-Z4). This is a surprising result at first: an increasing density could be expected as the density of fully densified ZrO_2 (5.86 g/cm^3)[29] is twice as high as that of SiO_2 (2.36 g/cm^3).[40,41] These measurements in fact strongly indicate that, as ZTP was introduced, on top of the inorganic network formation, the organic network was also greatly modified. In an attempt to understand how the ZTP changes the coatings chemical/structural composition, FTIR was performed on the different samples.

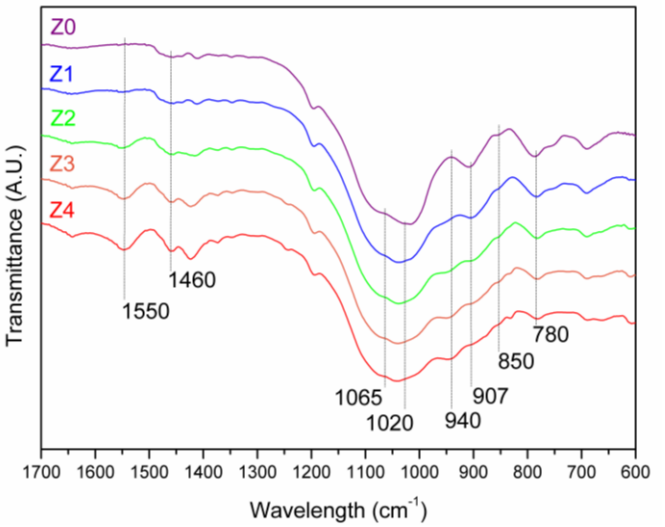

Fig 4 FT-IR spectra of PC-Z0, PC-Z1, PC-Z2, PC-Z3 and PC-Z4

Chemical network analysis by FTIR and ^{17}O MAS NMR

The nature of the chemical bonding in the different films was first investigated using FTIR and solid state ^{17}O MAS NMR spectroscopies. The IR ATR of PC-Z0, PC-Z1, PC-Z2, PC-Z3 and PC-Z4, recorded with an ATR mode, are shown in Figure 4. For all samples, the most intense bands are observed at 1020 cm^{-1} and 1065 cm^{-1} which correspond to the Si-O-Si asymmetric stretching mode.[41,42] As expected, their intensity decreases from PC-Z0 to PC-Z4 due to the decreasing relative amount of Si-O-Si bonds when more zirconia is introduced into the coatings. The band at 780 cm^{-1} is attributed to the Si-C bond of GPTMS[43] and follows the same trend as the Si-O-Si band. The presence of zirconia in the silica network is evidenced by the band at 940 cm^{-1}, indicative of Si-O-Zr bonds,[21] confirming the good incorporation of zirconia in the silica network through the formation of covalent bonds. PC-Z0 naturally doesn't display this band, but the band intensity gradually increases with the ZTP content, for the zirconia containing samples.[40]
The bands at 1460 cm^{-1} and 1560 cm^{-1} are due to the presence of MAA and attributed to symmetric and anti-symmetric –COO stretching, respectively.[44] Both bands increase in intensity from PC-Z1 to PC-Z4 as the MAA amount added to the sols is proportional to that of ZTP. According to the literature, MAA can coordinate with ZTP in two different modes: monodentate, chelating one ZTP molecule or bidentate, bridging two metal centers. In our case, the small difference in wavenumber between the two bands (100 cm^{-1}) suggests that the bidentate coordination mode prevailed.[44]

Lastly, the two bands at 850 cm^{-1} and 907 cm^{-1} can be ascribed to the asymmetrical epoxy ring stretching of GPTMS.[45] Unlike the band at 850 cm^{-1} that displays very low intensity and is difficult to follow from one sample to the next, the evolution of the band at 907 cm^{-1} shows a significant decrease in intensity from PC-Z0 to PC-Z4. When the ZTP content is high (as illustrated for PC-Z4), the band almost disappears, indicating that epoxy ring opening occurred and was almost complete.
FTIR therefore gives strong evidence of GPTMS epoxy ring opening in the formulations, due to the catalytic effect of ZTP. It was also observed that the number of opened epoxy groups increased with the ZTP quantity and that ring opening was almost complete for high ZTP content samples. As the epoxy groups open, they can react with each other or with silanols and hydrolyzed ZTP, forming a poly(ethylene oxide) network. This enhancement in organic network polymerization is responsible for the increase in coating's plasticity and plays an important role in the mechanical properties and scratch resistance improvement.
In order to evidence Zr-O-Zr bonds, solid state ^{17}O NMR was used. Figure 5 shows the ^{17}O NMR spectra for Z1-^{17}O, Z2-^{17}O, Z3-^{17}O and Z4-^{17}O. These data not only provided information on Zr-O-Zr bonds, but also on the inorganic network structure in general. All the spectra display a main signal at about 50 ppm, characteristic of Si-O-Si species,[46–49] which is in good agreement with the expected majority silica network present in the coatings. Another marked signal, at around 200 ppm, is present in all the spectra and corresponds to Si-O-Zr bonds.[46,48,49] The signal intensity increases with the ZTP content, indicative of the good incorporation of zirconia in the silica network through the formation of a more and more mixed network, which is in excellent agreement with the IR data (*vide supra*). Finally, these ^{17}O NMR spectra also show a signal at 400 ppm, attributed to the presence of Zr-O-Zr species.[46,48,49] Interestingly, this signal is only present for Z3 and Z4, indicating that for low ZTP content samples, Zr-O-Si bond formation is favored over Zr-O-Zr. These results thus strongly support the good mixing of silica and zirconia networks, leading to homogeneous coatings without segregation.

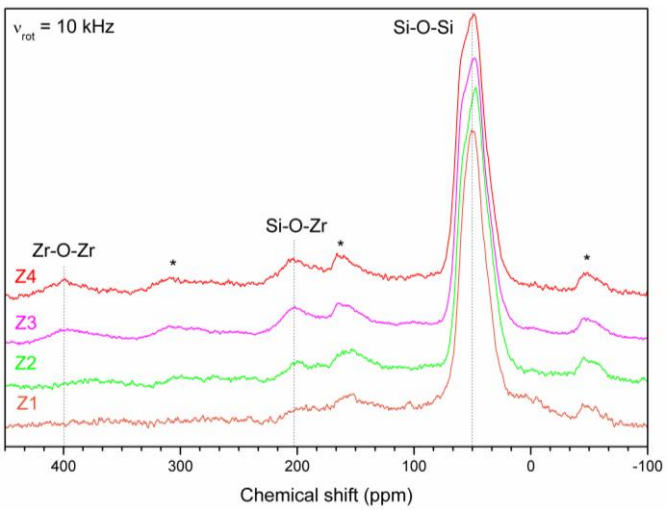

Fig 5 Solid state ^{17}O MAS NMR spectra of Z1-^{17}O, Z2-^{17}O, Z3-^{17}O and Z4-^{17}O samples recorded at 16.3 T (spinning sidebands are indicated with an asterisk)

Steam resistance

Lastly, simple steam resistance tests were carried out on the samples as zirconia is known to be highly resistant to hydrolysis. The coated PC samples were put into a chamber with 100% relative humidity and the time required for the water vapor to cause film delamination was measured. Water contact angle (WCA) measurements were preliminarily measured on all samples; the data can be found in Table 6.

Table 6 Steam resistance and contact angle of the different coatings

Sample	Time required for film delamination	Film contact angle
PC-Z0	5 min	65±0.4°
PC-Z1	20 min	65±0.6°
PC-Z2	2 h	80±0.3°
PC-Z3	12 h	90±0.4°
PC-Z4	18 h	95±0.2°

The results clearly indicate a better water vapor resistance for high ZTP content samples. It is worth noting that the water mainly penetrates the coatings from the top surface and not at the PC/film interface as similar delamination times for all samples (due to similar chemical interface, as suggested by their similar adhesion energy) would then be obtained. The difference in water vapor resistance is a direct consequence of the modifications in film composition induced by the ZTP and the MAA. It can be explained by i) the formation of Si-O-Zr and Zr-O-Zr bond that have a higher hydrolysis resistance as compared to Si-O-Si bonds[50] and ii) the presence of MAA that leads to more hydrophobic coatings, as observed by the WCA measurements. Hence, the addition of ZTP and MAA in the films have a beneficial effect on the hydrolysis resistance as they lead to modifications in organic and inorganic network that create a water vapor barrier which becomes more difficult to pass.

Conclusions

In conclusion, we have demonstrated that scratch-resistant coatings can be obtained by tuning the bulk structure and composition, despite poor film to substrate adhesion. This was achieved by adding zirconium (IV) propoxide in a 3-glycidoxypropyltrimethoxysilane based sol-gel formulation: concurrently to the formation of zirconia-type bonds, zirconium (IV) propoxide acts as a catalyst to open 3-glycidoxypropyltrimethoxysilane epoxy rings, leading to more polymerized organic domains. Consequently, significantly higher plasticity arises from the coating, resulting in a better resistance under scratch constraints. Lastly, the coatings steam resistance was also improved when the zirconium (IV) propoxide content was high. We believe that such transparent coatings with superior scratch resistance and high hydrophobicity, deposited onto polycarbonate, could greatly extend the substrate's lifetime while maintaining the initial transparency feature of polycarbonate in various applications such as windows, optical glasses or any other applications where transparency is a must.

Acknowledgements

This work was supported by the Programme Avenir Lyon Saint-Etienne (ANR-11-IDEX-0007) of Université de Lyon, within the program "Investissements d'Avenir" operated by the French National Research Agency (ANR) and the French Région Ile de France - SESAME program (700 MHz NMR spectrometer).

Notes and references

[a] *Laboratoire de Tribologie et Dynamique des Systèmes, Ecole Centrale de Lyon, Ecully, 69130, France*

[b] *Laboratoire des Multimatériaux et Interfaces, UMR 5615, Université de Lyon, Villeurbanne, 69622, France*

[c] *IBM Almaden Research Center, San Jose, California 95120, United States*

[d] *Sorbonne Universités, UPMC Univ Paris 06, CNRS, Collège de France, UMR 7574, Chimie de la Matière Condensée de Paris, 75005 Paris, France*

* klionti@us.ibm.com

* toury@univ-lyon1.fr

1 M. Diepens and P. Gijsman, *Polym. Degrad. Stab.*, 2007, **92**, 397–406.

2 M. Diepens and P. Gijsman, *Polym. Degrad. Stab.*, 2008, **93**, 1383–1388.

3 M. Diepens and P. Gijsman, *Polym. Degrad. Stab.*, 2011, **96**, 649–652.

4 G. Grause, N. Tsukada, W. J. Hall, T. Kameda, P. T. Williams and T. Yoshioka, *Polym. J.*, 2010, **42**, 438–442.

5 K. Lionti, B. Toury, C. Boissiere, S. Benayoun and P. Miele, *J. Sol-Gel Sci. Technol.*, 2013, **65**, 52–60.

6 I. Saaem, K.-S. Ma, S. M. Alam and J. Tian, *J. Vac. Sci. Technol. A*, 2010, **28**, 963–968.

7 J. M. Lackner, W. Waldhauser, M. Schwarz, L. Mahoney, L. Major and B. Major, *Vacuum*, 2008, **83**, 302–307.

8 D. Katsamberis, K. Browall, C. Iacovangelo, M. Neumann and H. Morgner, *Prog. Org. Coat.*, 1998, **34**, 130–134.

9 M. Shinoda, T. Nishide and Y. Shichi, *J. Vac. Sci. Technol. -Vac. Surf. Films*, 1994, **12**, 746–750.

10 J. Theil, D. Tsu, M. Watkins, S. Kim and G. Lucovsky, *J. Vac. Sci. Technol. -Vac. Surf. Films*, 1990, **8**, 1374–1381.

11 L. Cui, A. N. Ranade, M. A. Matos, G. Dubois and R. H. Dauskardt, *ACS Appl. Mater. Interfaces*, 2013, **5**, 8495–8504.

12 L. Cui, A. N. Ranade, M. A. Matos, L. S. Pingree, T. J. Frot, G. Dubois and R. H. Dauskardt, *ACS Appl. Mater. Interfaces*, 2012, **4**, 6587–6598.
13 L. Cui, K. Lionti, A. Ranade, K. Larson-Smith, G. J. Dubois and R. H. Dauskardt, *ACS Nano*, 2014, **8**, 7186–7191.
14 M. Dinelli, E. Fabbri and F. Bondioli, *J. Sol-Gel Sci. Technol.*, 2011, **58**, 463–469.
15 H. Yavas, C. D. O. Selcuk, A. E. S. Ozhan and C. Durucan, *Thin Solid Films*, 2014, **556**, 112–119.
16 M. V. Kahraman, G. Bayramoglu, Y. Boztoprak, A. Gungor and N. Kayaman-Apohan, *Prog. Org. Coat.*, 2009, **66**, 52–58.
17 Z. Altintas, S. Karatas, N. Kayaman-Apohan and A. Gungor, *Polym. Adv. Technol.*, 2011, **22**, 270–278.
18 M. E. L. Wouters, D. P. Wolfs, M. C. van der Linde, J. H. P. Hovens and A. H. A. Tinnemans, *Prog. Org. Coat.*, 2004, **51**, 312–320.
19 P. Fabbri, C. Leonelli, M. Messori, F. Pilati, M. Toselli, P. Veronesi, S. Morlat-Therias, A. Rivaton and J. L. Gardette, *J. Appl. Polym. Sci.*, 2008, **108**, 1426–1436.
20 P. Innocenzi, M. Esposto and A. Maddalena, *J. Sol-Gel Sci. Technol.*, 2001, **20**, 293–301.
21 P. Kiruthika, R. Subasri, A. Jyothirmayi, K. Sarvani and N. Y. Hebalkar, *Surf. Coat. Technol.*, 2010, **204**, 1270–1276.
22 G. Philipp and H. Schmidt, *J. Non-Cryst. Solids*, 1986, **82**, 31–36.
23 K. Lionti, L. Cui, W. Volksen, R. Dauskardt, G. Dubois and B. Toury, *Acs Appl. Mater. Interfaces*, 2013, **5**, 11276–11280.
24 G. I. Spijksma, H. J. M. Bouwmeester, D. H. A. Blank and V. G. Kessler, *Chem. Commun.*, 2004, 1874–1875.
25 S. Roche, S. Pavan, J. L. Loubet, P. Barbeau and B. Magny, *Prog. Org. Coat.*, 2003, **47**, 37–48.
26 L. Y. L. Wu, E. Chwa, Z. Chen and X. T. Zeng, *Thin Solid Films*, 2008, **516**, 1056–1062.
27 E. Roussi, A. Tsetsekou, A. Skarmoutsou, C. A. Charitidis and A. Karantonis, *Surf. Coat. Technol.*, 2013, **232**, 131–141.
28 M. Giachino, G. Dubois and R. H. Dauskardt, *ACS Appl. Mater. Interfaces*, 2013, **5**, 9891–9895.
29 K. Hara and M. Imanaka, *Tetsu Hagane-J. Iron Steel Inst. Jpn.*, 2007, **93**, 296–302.
30 H. Pelletier, C. Mendibide and A. Riche, *Prog. Org. Coat.*, 2008, **62**, 162–178.
31 L. Sowntharya, S. Lavanya, G. R. Chandra, N. Y. Hebalkar and R. Subasri, *Ceram. Int.*, 2012, **38**, 4221–4228.
32 H. Yahyaei and M. Mohseni, *Tribol. Int.*, 2013, **57**, 147–155.
33 Z. He, Z. Jue-Hui, Z. Qi-Long and Y. Hui, *J. Inorg. Mater.*, 2013, **28**, 785–789.
34 A. Leyland and A. Matthews, *Wear*, 2000, **246**, 1–11.
35 E. Le Bourhis, P. Goudeau, M. H. Staia, E. Carrasquero and E. S. Puchi-Cabrera, *Surf. Coat. Technol.*, 2009, **203**, 2961–2968.
36 S. Valette and S. Benayoun, *Appl. Surf. Sci.*, 2013, **279**, 62–66.
37 S. Bec, A. Tonck and J. L. Loubet, *Philos. Mag.*, 2006, **86**, 5347–5358.
38 S. Pellice, U. Gilabert, C. Solier, Y. Castro and A. Duran, *J. Non-Cryst. Solids*, 2004, **348**, 172–179.
39 N. C. Rosero-Navarro, S. A. Pellice, Y. Castro, M. Aparicio and A. Durán, *Surf. Coat. Technol.*, 2009, **203**, 1897–1903.
40 Z. G. Wu, Y. X. Zhao and D. S. Liu, *Microporous Mesoporous Mater.*, 2004, **68**, 127–132.
41 J. Y. Bae, S. Yang, J. H. Jin, K. Jung, J. S. Kim and B. S. Bae, *J. Sol-Gel Sci. Technol.*, 2011, **58**, 114–120.
42 C. J. Fu, Z. W. Zhan, M. Yu, S. M. Li, J. H. Liu and L. Dong, *Int. J. Electrochem. Sci.*, 2014, **9**, 2603–2619.
43 E. Nouri, M. Shahmiri, H. R. Rezaie and F. Talayian, *Surf. Coat. Technol.*, 2011, **205**, 5109–5115.
44 M. Ochi, D. Nii and M. Harada, *J. Mater. Sci.*, 2010, **45**, 6159–6165.
45 S. Senani, E. Campazzi, M. Villatte and C. Druez, *Surf. Coat. Technol.*, 2013, **227**, 32–37.
46 B. Julian, C. Gervais, M. N. Rager, J. Maquet, E. Cordoncillo, P. Escribano, F. Babonneau and C. Sanchez, *Chem. Mater.*, 2004, **16**, 521–529.
47 C. Gervais, F. Babonneau and M. E. Smith, *J. Phys. Chem. B*, 2001, **105**, 1971–1977.
48 C. Guermeur, J. Lambard, J. F. Gerard and C. Sanchez, *J. Mater. Chem.*, 1999, **9**, 769–778.
49 S. E. Ashbrook and M. E. Smith, *Chem. Soc. Rev.*, 2006, **35**, 718–735.
50 M. A. Villegas, *Thin Solid Films*, 2001, **382**, 124–132.